Methods:

Immunoblot analysis: Whole cell lysates were prepared using RIPA lysis buffer (10 mM Tris HCl, pH 8.0, 1mM EDTA, 150 mM NaCl, 1% Triton-X-100, 0.1% sodium deoxycholate, 0.1% SDS) in the presence of 1X Halt protease inhibitor (Thermo Fisher) and 1 mM PMSF (Sigma, St Louis, MA). The resulting proteins were resolved on an SDS-PAGE gel and the proteins were then transferred to nitrocellulose membrane for immune blotting. The membranes were incubated with protein-specific primary antibodies overnight at 4°C followed by incubation with HRP-tagged anti-mouse or anti-rabbit secondary antibodies for 1 hour at room temperature. An enhanced chemiluminescence kit (Thermo Fisher, Waltham, MA) was used to detect the immuno-reactive bands. The primary antibodies purchased from Cell-Signaling Technology (Danvers, MA) include pRB S807/811 (8516S), PS6 (S235/236) (2211S), S6 (2217S), CDK2 (2546S), CDK4 (12790S), PARP (9542S), γH2AX (S139) (9966S), Cyclin D1 (55506S), cyclin B1 (12231S), cyclin E1 (4129S), c-IAP1 (7065S). Cyclin A (SC271682), CDK1 (SC-54), WEE1 (SC-5285), β Actin (SC47778) and GAPDH (SC-47724) were purchased from Santacruz Biotech, Dallas, TX. Anti-phospho-p130 (S672) antibody was purchased from Abcam (ab-76255). AURKA antibody was purchased from R&D systems (Cat # AF3295). Mouse-IgGκ-HRP (Santacruz; SC516102) and Goat-anti-rabbit-HRP (Thermo Fisher; 31460) were used as secondary antibodies. An enhanced chemiluminescent substrate (National Diagnostics; CL-300) was used to detect the immunoreactive bands.

***In vitro* kinase reactions:** The CDK2 kinase activity from MCF7 and T47D cells was determined by immunoprecipitating CDK2 complexes from the whole lysates. Cells were lysed with kinase - lysis buffer containing 50 mM HEPES-KOH pH7.5, 150 mM NaCl, 1 mM EDTA, 1 mM DTT, 0.1% Tween-20 in the presence of 1x Halt protease inhibitor (Thermo Fisher) and 1 mM PMSF. Active CDK2 complex was immunoprecipitated by incubating the whole cell lysate (300 µg) with5 µg of anti-CDK2 antibody (SC6248, Santacruz Biotechnology) overnight at 4°C. Normal mouse

IgG (Cell signaling Technology, 5415S) was used an isotype control. Protein G-agarose beads were added to each of the IP samples and incubated up to 4 hours at 4°C. Following immunoprecipitation, the complexes were washed 3 times with the kinase-lysis buffer and 2 times with the kinase-reaction buffer (40 mM Tris-HCl pH 8, 20 mM $MgCl_2$, 0.1 mg/mL BSA, 50 µM DTT). Kinase reactions were carried out in the presence of 200 µM ATP and 0.5 µg of recombinant RB C-terminal as substrate [1]. The resulting RB phosphorylation was detected by western blotting using anti-pRB (S780) antibody (Cell Signaling, 9307L).

Immunofluorescence: Cells were seeded on glass coverslips and exposed to experimental drugs for 48 H. Cells were washed using 1X PBS, fixed in methanol and permeabilized in 0.5% Triton X-100. The permeabilized cells were blocked using IF buffer (1X PBS, 5% BSA, 0.4% NP40) and then incubated with the primary antibody, anti-γH2AX (S139) (Cell Signaling Technology; SC-9966) and phospho-histone H3 (Millipore Sigma), RB4H1 (Cell signaling Technology; 9309L) at room temperature for 1 h. Following primary antibody incubation, the cover slips were washed in PBS and then incubated in secondary antibody in the presence of DAPI for nuclear staining. Cover slips were washed again in PBS after secondary antibody incubation and mounted on glass slides. Pictures were taken using EVOS fluorescence microscope at 40X magnification.

Flow Cytometry Cell-cycle analysis: Cells that were treated with MK1775 and Alisertib up to 48 h were pulsed with BrdU for 4 h before harvesting. Cells were trypsinized and fixed in 70% ethanol overnight at -20°C. Collected cell pellets were washed with IFA buffer (1X PBS, 0.1 M sodium tetraborate (pH 8.5), 2 N HCl, 0.5% Triton X-100) and washed again with the IFA wash buffer (IFA + 1% BSA). Cell pellets were then incubated in FITC-conjugated anti-BrdU (BD Pharmingen) in antibody dilution buffer (1X PBS, 0.5% Tween

20, 1% BSA) up to 1h at room temperature. Cells were then resuspended in propidium iodide and RNaseA prior to analysis using BD LSRFORTESSA flow cytometer. BrdU incorporation was analyzed using the FCS express software and the population of cells at each phase of the cell-cycle were graphed using GraphPad Prism 7. Data were considered based on three independent experiments.

Immunofluorescent staining and imaging: Immunofluorescence on tumor tissues was performed following formalin fixation using the standard procedures with pRB S807/811 (Cells Signaling; 8516S). Staining was done on a Leica auto-stainer and image processing was performed using Aperio (Leica Biosystems).

Supplementary figure legends

Fig. S1. PIK3CA mutation status from MCF7 and T47D cells that has been analyzed using IGV based on RNA sequencing data.

Fig. S2. (A) Representative image of T47D cells stably expressing H2B-GFP. (B) Scatter plot indicating the correlation of relative growth rate from two independent drug screens. The R^2 and p-values were indicated. (C) PCA analysis from MCF7 and T47D cells that were treated with 2 different concentrations of the 305-drug library. (D) Heat map generated based on PCA analysis. (E) List of PI3K, mTOR and Akt inhibitors that are highly enriched in cluster 1. (F) IC50 values for alpelisib in MCF7 and T47D cells. Column represents mean from triplicates. Experiment was done at 2 independent times. (***$p<0.001$ as determined student t-test).

Fig. S3. (A) Effect of CCND1 knockdown on the proliferation of MCF7 and T47D cells based on live cell imaging. Error bars represent mean and SD from triplicates. Experiments were performed at two independent times. (B) Western blot to evaluate cyclin D1 expression following the KD using gene specific RNAi (12.5 nM). (C) Effect of palbociclib (50 nM) in combination with alpelisib (125 nM) on the indicated proteins from MCF7-WT and MCF7-D1/K4 cells following 48 H

treatment. (D) Western botting on the indicated proteins from T47D and T47D-D1/K4 cells that were exposed to palbociclib +/- alpelisib at the indicated concentration for 48 H. (E) Live cell imaging to determine the proliferation of MCF7-WT and MCF7-D1/K4 cells following the treatment with fulvestrant (100 nM) in combination with ipatasertib (125 nM) and GSK690693 (125 nM). Error bars represent mean and SD from triplicates. Experiments were performed at two independent times. (F) Effect of fulvestrant (100 nM) in combination with everolimus (125 nM) and alpelisib (125 nM) on the proliferation of MCF7-RB-del cells. Following 6-days of treatment the drug was removed and the cell growth was monitored for another 4 days. Error bars represent mean and SD from triplicates. Experiments were performed at two independent times.

Fig. S4. (A) Volcano plots from gene expression analysis to indicate the up regulated and down regulated genes from MCF7-WT and MCF7-RB-del cells treated with palbociclib +/- everolimus. (B) ENRICHR analysis to represent the top gene ontology sets that were significantly suppressed in MCF7-WT and MCF7-RB-del cells treated with Palbo/Evero based on RNA sequencing analysis. (C) Heat map analysis that represent the differential expression of genes involved in multiple signaling pathways from MCF7-WT and RB-del cells that were treated with palbo/evero. (D) Relative mRNA expression of representative cell cycle genes in MCF7-WT and RB-del cells treated with palb/evero. Graphs represent mean and SD from two independent runs (* $p<0.5$, **$p<0.01$ as determined student t-test. (E) Western blot analysis on T47D-WT and RB-del cells that were treated with palbociclib +/- everolimus for 48H at the indicated concentration.

Fig. S5. (A) Contour plots that represent the relative BrdU incorporation from T47D WT, T47D-RB-del, MCF7-WT and MCF7-RB-del cells that were treated with different concentrations of palbociclib in combination with different concentrations of everolimus and alpelisib. The synergy scores were calculated based on the Bliss method. (B) Column graph represents the relative BrdU incorporation from T47D WT, T47D-RB-del, MCF7-WT and MCF7-RB-del cells in the presence of palbociclib +/- everolimus/alpelisib at the indicated concentrations. Mean and SD were

calculated from triplicates. (* p<0.1, ** p<0.05, ***p<0.001 as determined by t-test). (C) Relative BrdU incorporation from CAMA-1 cells that were treated with different concentrations of alpelisib up to 72 H. Error bars represent mean and SD from triplicates. (D). Immunofluorescence to determine the RB expression from CAMA-1 WT and CAMA-1-RB-del cells. (E) Western blot analysis on RB expression from CAMA-1 WT and CAMA-1-RB-del cells.

Fig S6: Table illustrating the clinical characteristics of patients who harbor wild-type RB1 (n=68) and RB1-deletion mutation (n=3) based on genetic testing.

Fig. S7 (A) Scatter plot analysis to determine the correlation of basal expression of genes involved in cell cycle and ER pathways between wild-type and RB del samples from both MCF7 and T47D cells. (B) Heat maps representing the normalized read counts of genes involved in cell cycle and ER pathways from both MCF7 and T47D WT/RB-del cells. (C) Basal expression of the indicated proteins from MCF7-WT, MCF7-RB-del, T47D-WT and T47D-RB-del cells. (D) Basal cell proliferation of MCF7-WT, MCF7-RB-del, T47D-WT and T47D-RB-del cells based on live cell imaging.

Fig. S8 (A) *In vitro* kinase assay to determine the activity of CDK2 in the presence of exogenous C-terminus RB as a substrate on T47D-WT and RB-del cells treated with palbo/evero for 48H. CDK2 was immunoprecipitated and the co-immunoprecipitated proteins were detected by western blotting. Densitometry was performed to quantify the intensity of pRB as a measure of CDK2 kinase activity and plotted in a column graph. Mean and SD were calculated from 2 independent experiments. (** p<0.05 as determine by t-test). (B) Live cell imaging to monitor the CDK2 kinase activity based on the localization of the CDK2 sensor in T47D-WT and T47D-RB-del cells that were treated with Palbo/Evero. Scale bar represents 50 µm.

Fig. S9. (A) Heat map from drug screen analysis that indicate the differential effect of drugs from cluster 2 on the proliferation of MCF7-WT and MCF7-RB-del cells. (B) List of drugs from cluster

2 and their corresponding cellular targets. (C) Scatter plot representing the correlation of the viability of MCF7-RB-del cells normalized to MCF7-WT cells from two independent experiments. R^2 and p values were indicated.

Fig. S10. Contour plots that represent the relative cell viability of MCF7-WT and MCF7-RB-del cells that were treated with different pairwise combinations of the indicated drugs. The synergy scores were calculated based on the Bliss method. (B) Column graph indicates the densitometry analysis of cleaved PARP from MCF7-WT/RB-del and T47D-WT/RB-del cells following the knockdowns of AURK1 and WEE1. Error bars represent SEM from 2 independent experiments (** $p<0.05$ as determined by one-way ANOVA).

Fig. S11. (A) Immunofluorescence staining for phospho-histone H3 (S10) in MCF7-WT and RB-del cells that were treated with MK1775 (200 nM) in combination with Alsiertib (200 nM) at the indicated time points. (B) Representative flow cytometry analysis of MCF7-WT and RB-del cells treated with Alisertib (200 nM) and MK1775 (200 nM) for 48 H. X and Y axis represent DNA content and BrdU incorporation respectively. Quantification of 4N cells that were stained positive for BrdU from MCF7 and T47D WT/RB-del cells. The mean and SD are shown from 3 different experiments (**$p<0.01$ and ***$p<0.001$ as determined by student t-test). (C) Cell cycle profile of T47D and MCF7 WT/ RB-del cells that were treated with MK1775 (200 nM) in combination with Alsiertib (200 nM) up to 48 H. (D) Immunofluorescence staining for γ-H2AX in T47D-WT and RB-del cells that were treated with pemetrexed (100 nM) in combination with CHIR 124 (100 nM) up to 48 H. (E) Western blot analysis on the indicated proteins from T47D-WT and RB-del cells following 48 H exposure with pemetrexed (100 nM) in combination with CHIR 124 (100 nM).

Fig. S12. (A) Immunofluorescence staining for pRB (S807/811) from tumors excised from MCF7-WT and RB-del xenografts. Scale bar represents 20 μm. (B) Western blot analysis on the indicated proteins from the tumor tissues excised from MCF7-WT and RB-del xenografts. (C) Representative images of tumors from MCF7-WT and RB-del xenografts that were treated with

vehicle and MK1775 in combination with alisertib. (D) Flow cytometry analysis of T47D-WT and RB-del cells treated with aphidicolin (1 µg/ml) in combination with Alisertib (200 nM) and MK1775 (200 nM) for 48 H. X and Y axis represent DNA content and BrdU incorporation respectively. (E) Western blotting to determine PARP cleavage from T47D-WT and RB-del cells following the treatment with aphidicolin (1 µg/ml) in combination with Alisertib (200 nM) and MK1775 (200 nM) for 48 H.

Fig. S13. (A) Scatter plot with X and Y axis representing the viability of MCF7-WT and RB-deleted cells respectively in the presence of each drug from the library. (B) Column graph indicates the densitometry analysis of cleaved PARP from MCF7-WT/RB-del and T47D-WT/RB-del cells treated with birinapant for 48 H. Error bars represent SEM from 3 independent experiments (** $p<0.05$ as determined by one-way ANOVA). (C) Volcano plot analysis from MCF7-WT and RB-del cells that were treated with birinapant (500 nM) up to 48 H to represent the differentially expressed genes. (D) Dot plot representing the differential upregulation of genes by birinapant (500 nM) in MCF7-WT and RB-del cells that are highly significant. (E) Heat map indicating the cell viability from drug screen analysis in MCF7-WT, MCF7-RB-del, T47D-WT and T47D-RB-del cells that were pretreated with birinapant (250 nM).

1. Knudsen, E.S. and J.Y. Wang, *Differential regulation of retinoblastoma protein function by specific Cdk phosphorylation sites.* J Biol Chem, 1996. **271**(14): p. 8313-20.

MCF7 PIK3CA (1633 G>A)

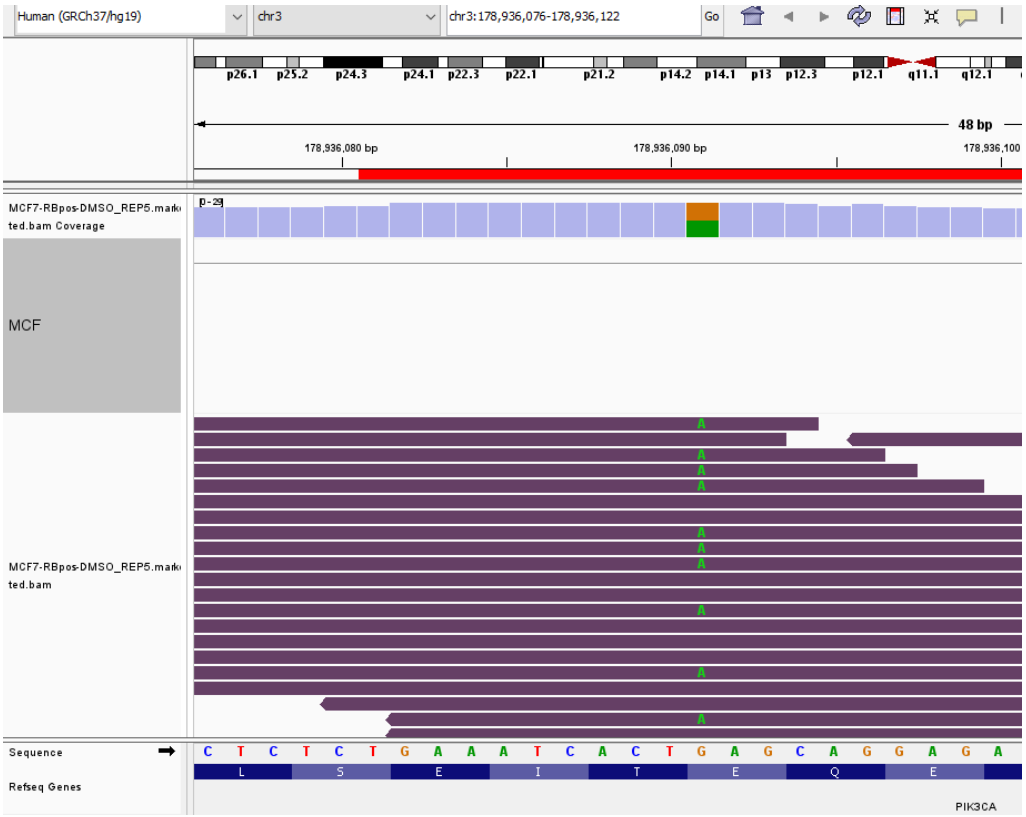

T47D PIK3CA (3140 A>G)

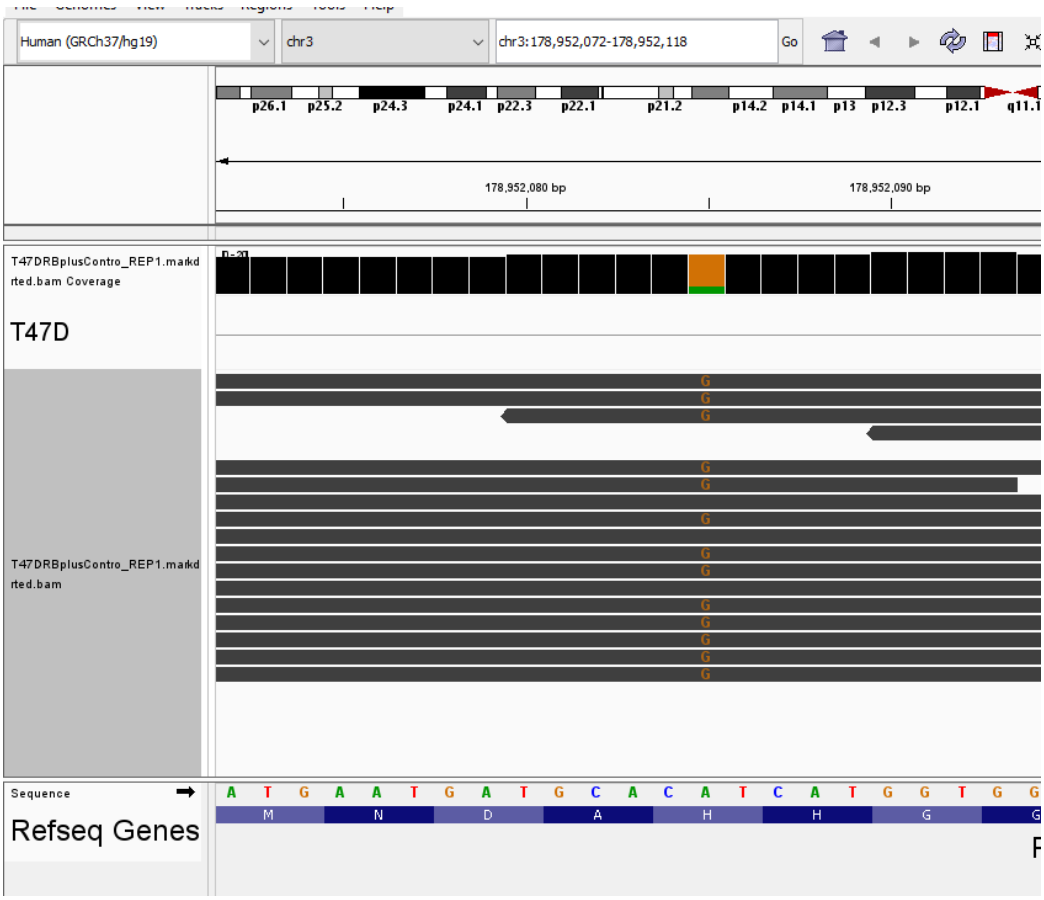

A

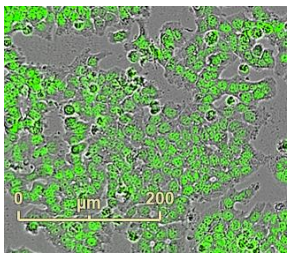

B

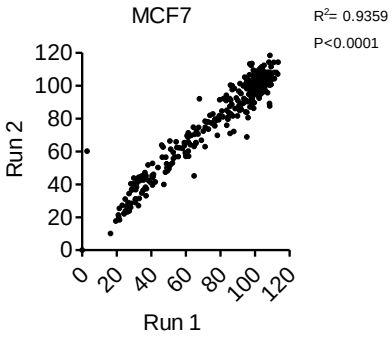

C

D

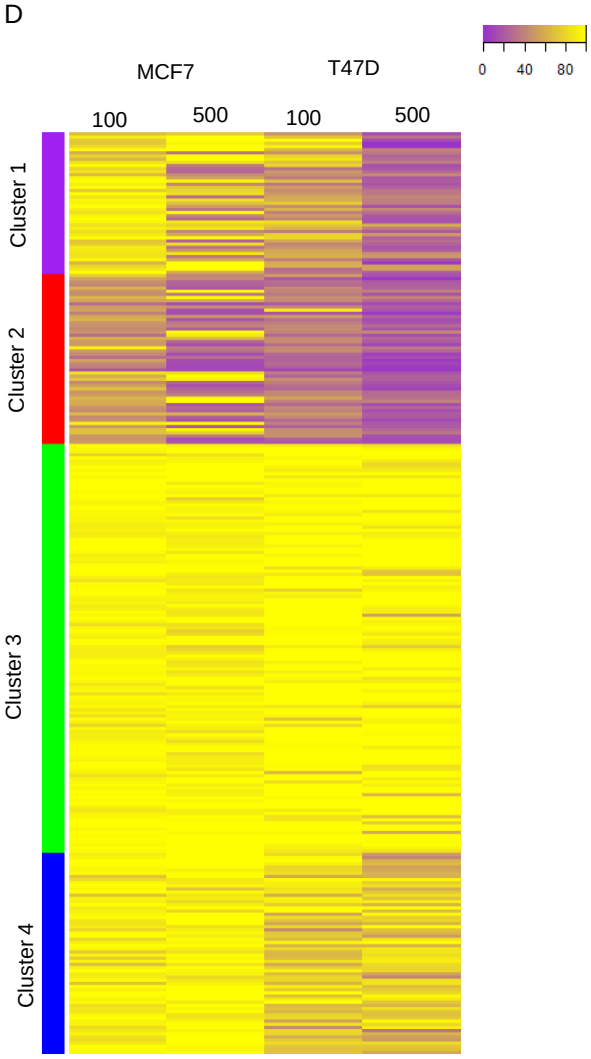

E

Cluster 1

Drugs	Target
PI-103	DNA-PK,mTOR,Autophagy,PI3K
KU-0063794	mTOR
WAY-600	mTOR
Rapamycin (Sirolimus)	mTOR
PP121	PDGFR,mTOR,DNA-PK
Everolimus (RAD001)	mTOR
GSK1059615	PI3K,mTOR
Torkinib (PP242)	mTOR,Autophagy
Temsirolimus (CCI−779, NSC 683864)	mTOR
WYE-354	mTOR

Drugs	Target
PIK-93	PI3K
Pictilisib (GDC-0941)	PI3K
BKM120 (NVP−BKM120, Buparlisib)	PI3K
Alpelisib (BYL719)	PI3K
ZSTK474	PI3K

Drugs	Target
A-674563	PKA,CDK,Akt
MK-2206 2HCl	Akt
Ipatasertib (GDC-0068)	Akt
GSK690693	Akt

F

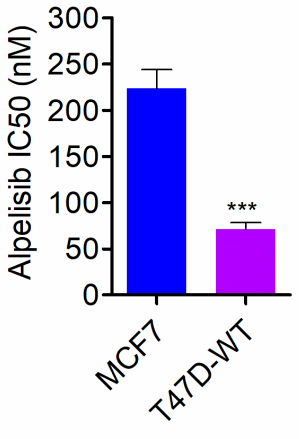

A

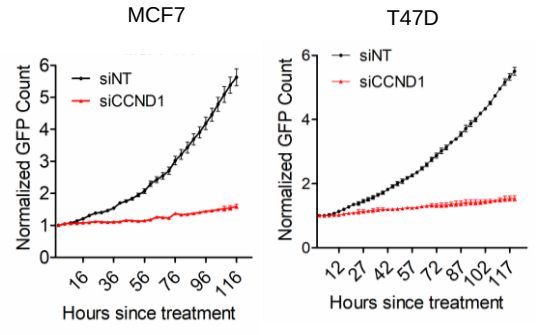
MCF7
T47D
siNT
siCCND1
Normalized GFP Count
Hours since treatment

B

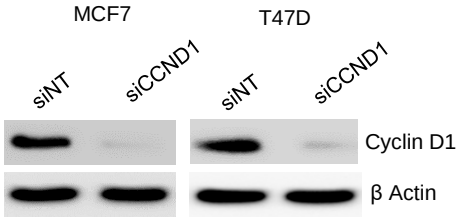
MCF7
T47D
siNT
siCCND1
siNT
siCCND1
Cyclin D1
β Actin

C

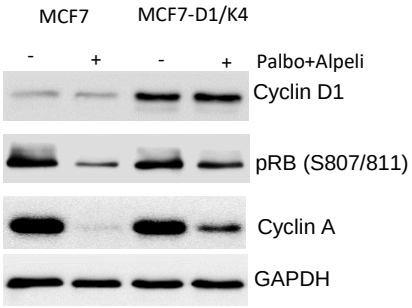
MCF7
MCF7-D1/K4
Palbo+Alpeli
Cyclin D1
pRB (S807/811)
Cyclin A
GAPDH

D

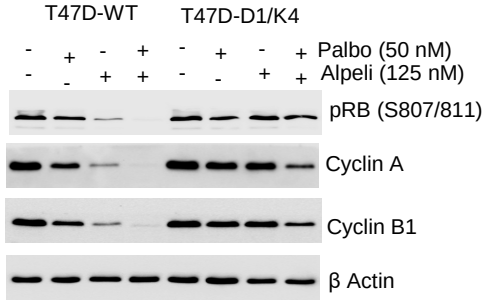
T47D-WT
T47D-D1/K4
Palbo (50 nM)
Alpeli (125 nM)
pRB (S807/811)
Cyclin A
Cyclin B1
β Actin

E

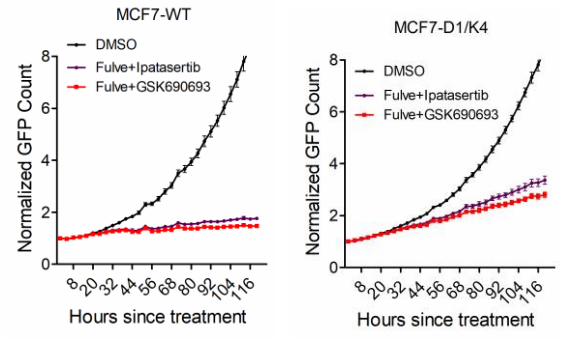
MCF7-WT
MCF7-D1/K4
DMSO
Fulve+Ipatasertib
Fulve+GSK690693
Normalized GFP Count
Hours since treatment

F

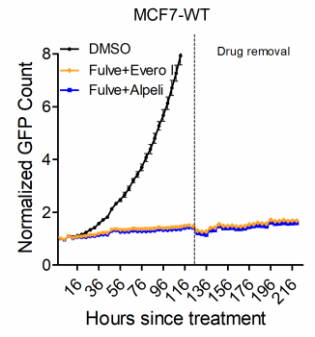
MCF7-WT
DMSO
Fulve+Evero
Fulve+Alpeli
Drug removal
Normalized GFP Count
Hours since treatment

Fig S4

A

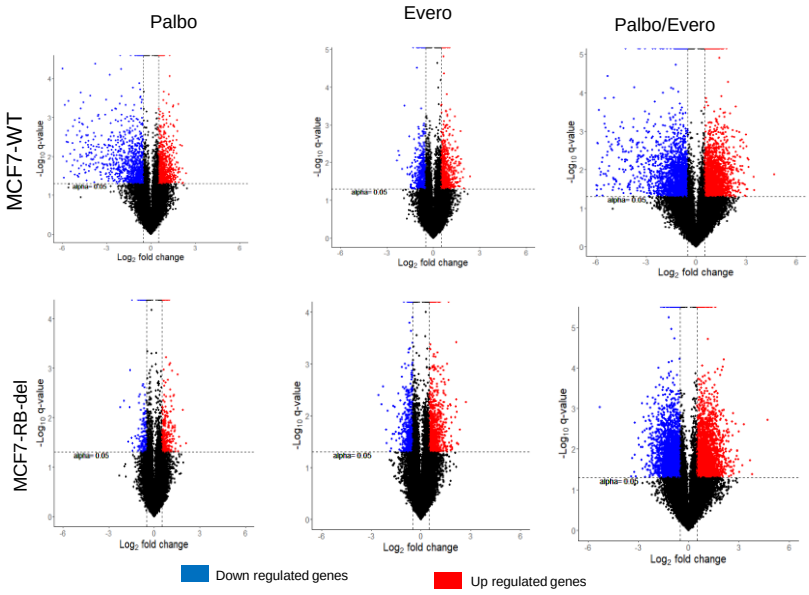
Palbo
Evero
Palbo/Evero
MCF7-WT
MCF7-RB-del
Log2 fold change
Down regulated genes
Up regulated genes

B

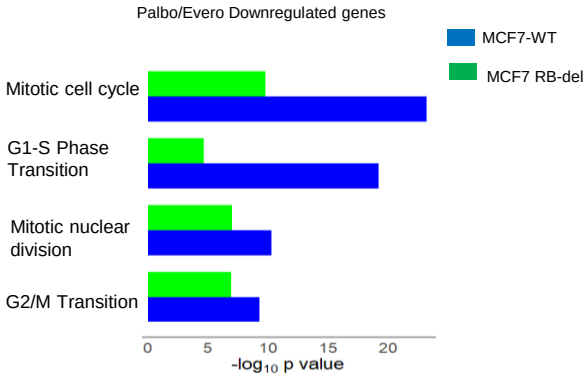
Palbo/Evero Downregulated genes
MCF7-WT
MCF7 RB-del
Mitotic cell cycle
G1-S Phase Transition
Mitotic nuclear division
G2/M Transition
-log10 p value

C

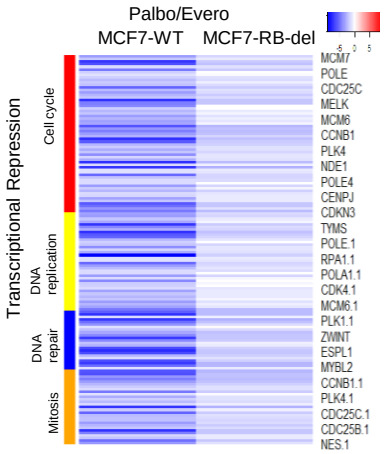
Palbo/Evero
MCF7-WT
MCF7-RB-del
Transcriptional Repression
Cell cycle
DNA replication
DNA repair
Mitosis
MCM7
POLE
CDC25C
MELK
MCM6
CCNB1
PLK4
NDE1
POLE4
CENPJ
CDKN3
TYMS
POLE.1
RPA1.1
POLA1.1
CDK4.1
MCM6.1
PLK1.1
ZWINT
ESPL1
MYBL2
CCNB1.1
PLK4.1
CDC25C.1
CDC25B.1
NES.1

D

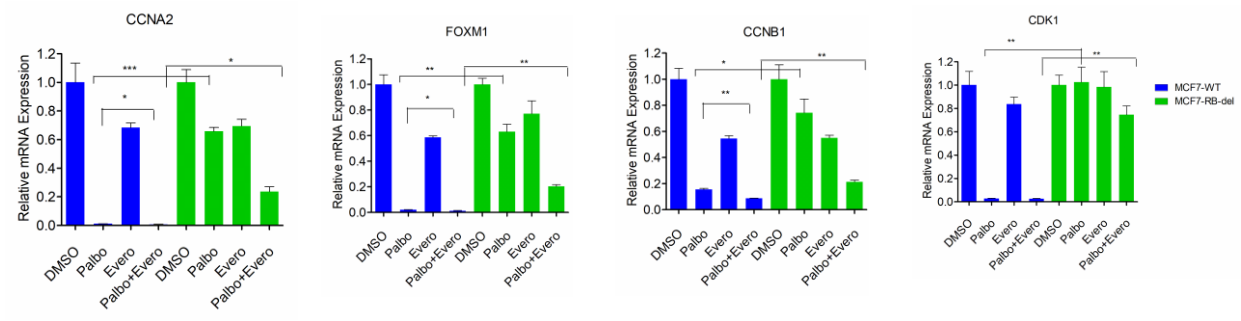
CCNA2
FOXM1
CCNB1
CDK1
Relative mRNA Expression
DMSO
Palbo
Evero
Palbo+Evero
MCF7-WT
MCF7-RB-del

E

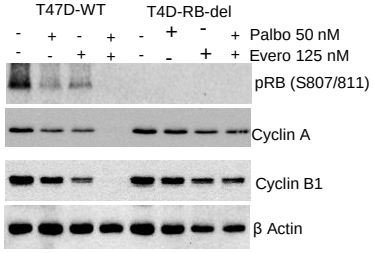
T47D-WT
T4D-RB-del
Palbo 50 nM
Evero 125 nM
pRB (S807/811)
Cyclin A
Cyclin B1
β Actin

Fig S5

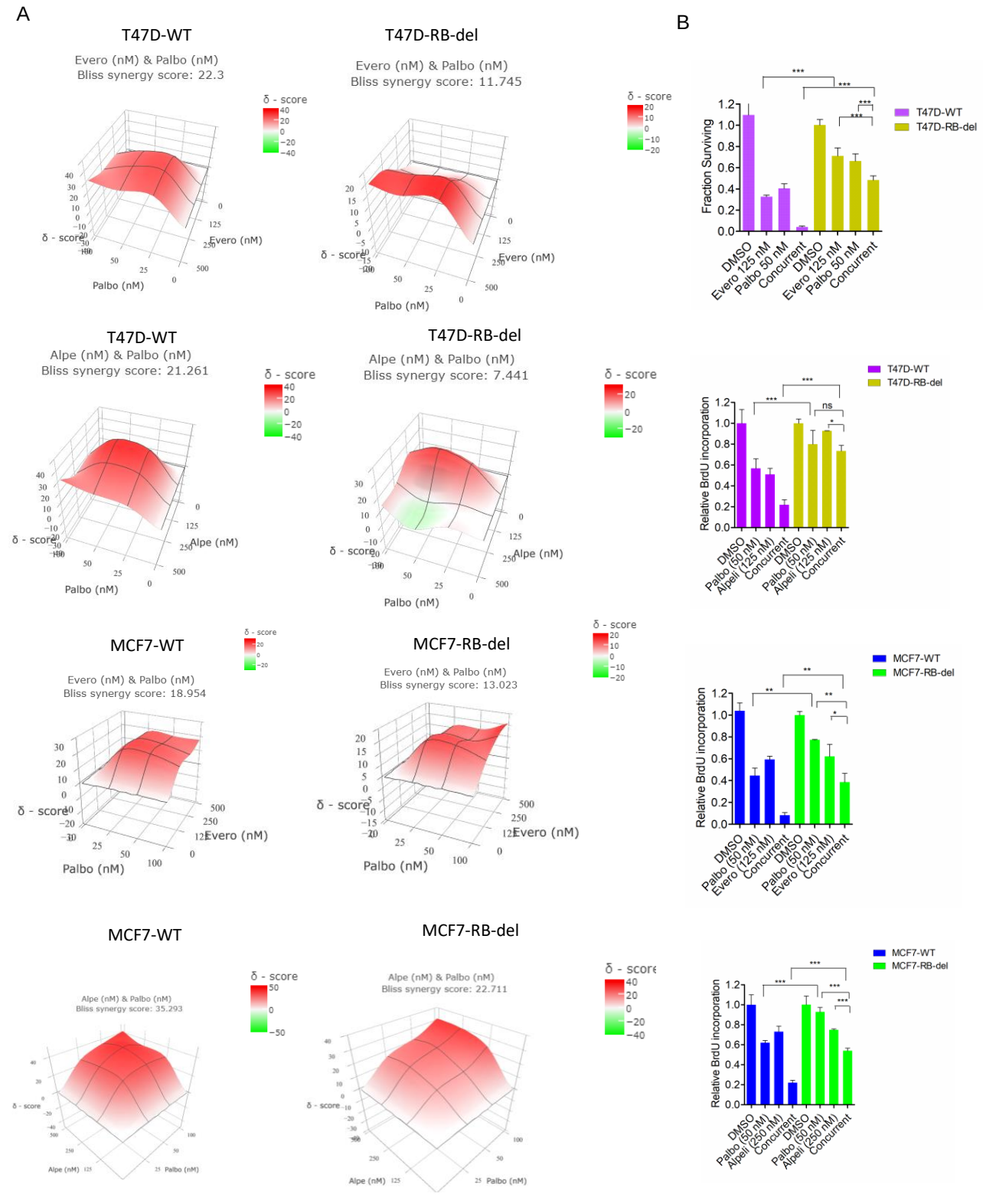
A
T47D-WT
Evero (nM) & Palbo (nM)
Bliss synergy score: 22.3
T47D-RB-del
Evero (nM) & Palbo (nM)
Bliss synergy score: 11.745
δ - score
Palbo (nM)
Evero (nM)
B
Fraction Surviving
T47D-WT
T47D-RB-del
DMSO
Evero 125 nM
Palbo 50 nM
Concurrent
Alpe (nM) & Palbo (nM)
Bliss synergy score: 21.261
Bliss synergy score: 7.441
Alpe (nM)
Relative BrdU incorporation
Palbo (50 nM)
Alpeli (125 nM)
MCF7-WT
MCF7-RB-del
Bliss synergy score: 18.954
Bliss synergy score: 13.023
Alpeli (250 nM)
Bliss synergy score: 35.293
Bliss synergy score: 22.711
C
CAMA-1
Alpeli (nM)
D
CAMA1-WT
CAMA1-RB-del
RB
DAPI
E
CAMA-1 WT
CAMA-1 RB-del
RB
β Actin

Fig S6

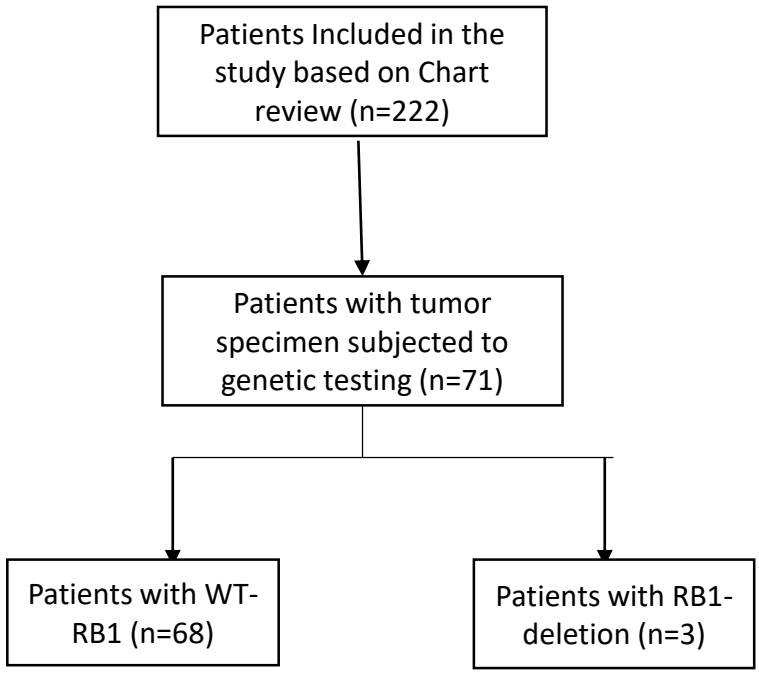

Characteristics	RB1-WT	RB1-Loss
Age at diagnosis		
<50	n=31	n=1
50 and older	n=37	n=2
Metastatic Status		
Recurrent	n=45	n=3
Denovo	n=23	
Metastatic site		
Visceral	n=30	n=3
Non-visceral	n=38	
PIK3CA status		
Wild-type	n=40	n=2
Mutant	n=27	n=1
NA	n=1	
TP53 status		
WT	n=59	n=1
Mutant	n=9	n=2
CDK4/6i		
Palbociclib	n=65	n=3
Ribociclib	n=2	
Abemaciclib	n=1	
Endocrine therapy		
Aromatase Inhibitor	n=49	n=2
Fulvestrant	n=18	n=1
Tamoxifen	n=1	

A

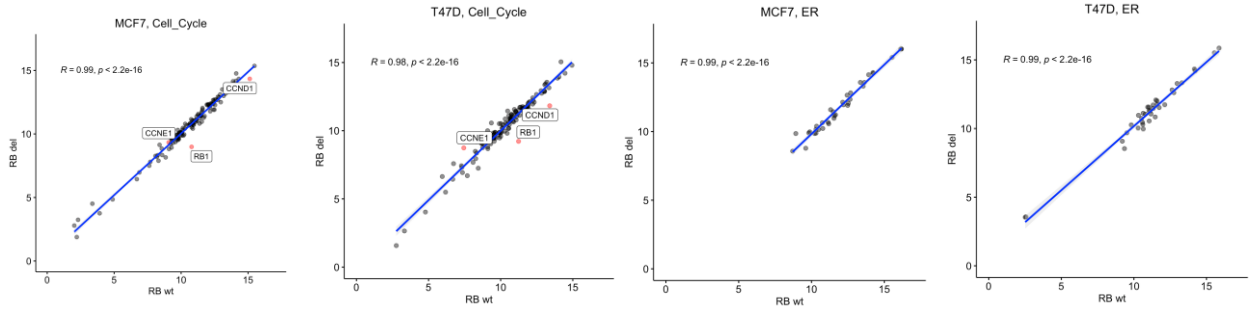
MCF7, Cell_Cycle
T47D, Cell_Cycle
MCF7, ER
T47D, ER
RB del
RB wt
CCND1
CCNE1
RB1

B

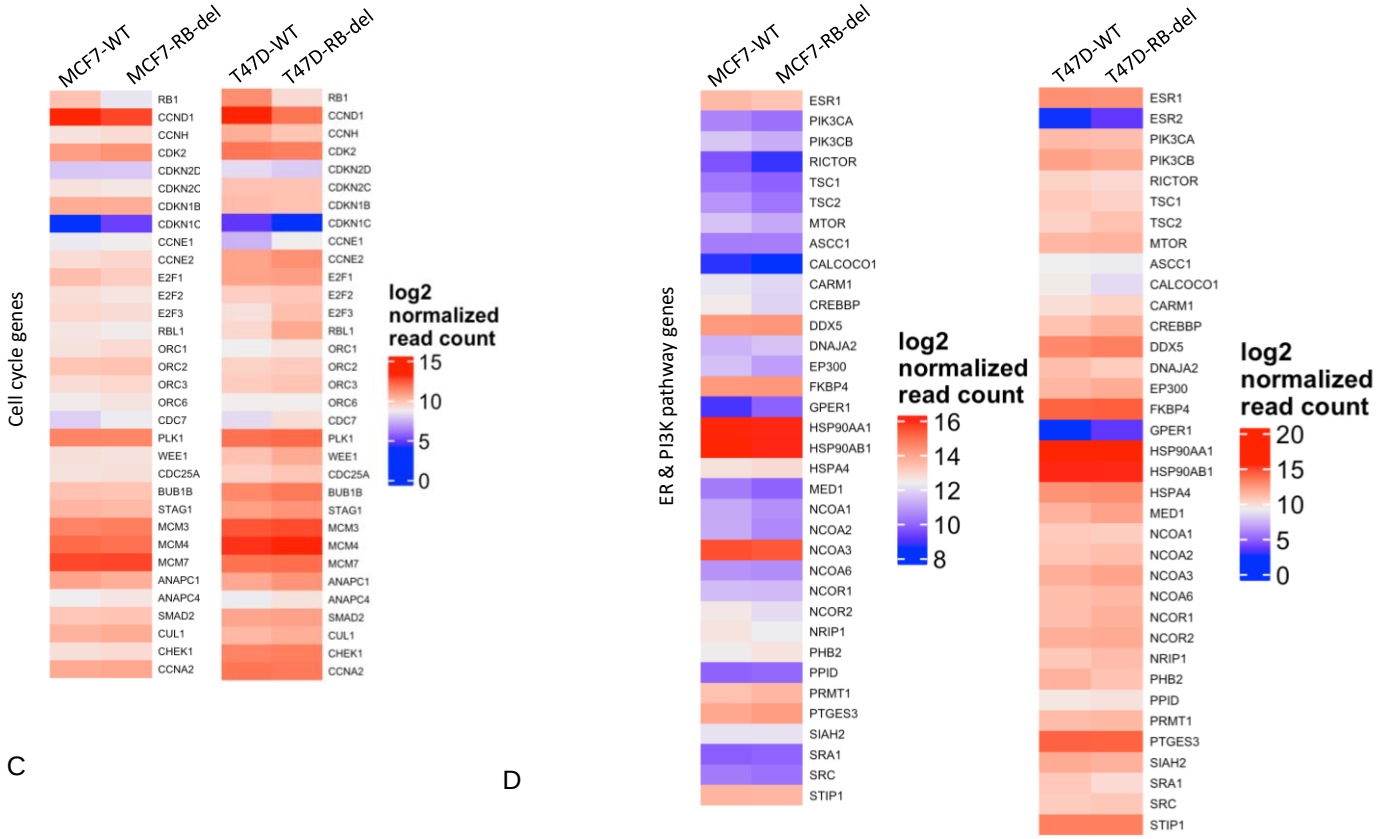
MCF7-WT
MCF7-RB-del
T47D-WT
T47D-RB-del
Cell cycle genes
ER & PI3K pathway genes
log2 normalized read count

C

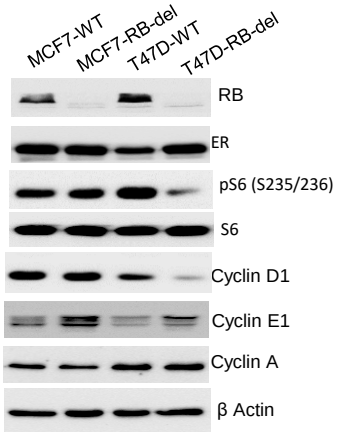
MCF7-WT
MCF7-RB-del
T47D-WT
T47D-RB-del
RB
ER
pS6 (S235/236)
S6
Cyclin D1
Cyclin E1
Cyclin A
β Actin

D

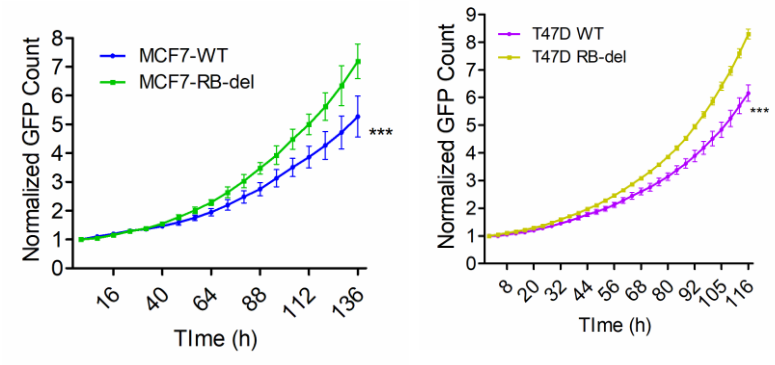
MCF7-WT
MCF7-RB-del
T47D WT
T47D RB-del
Normalized GFP Count
TIme (h)
***

A

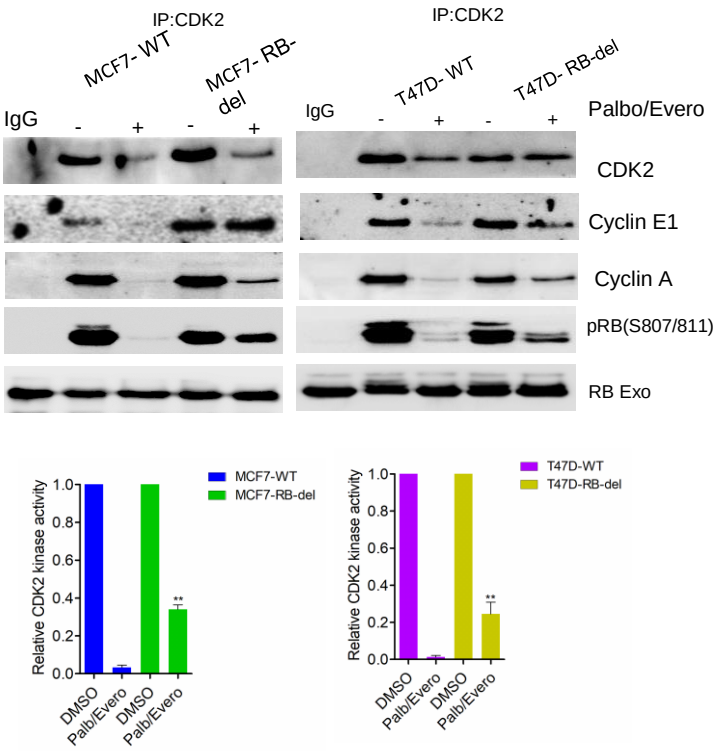
IP:CDK2
MCF7- WT
MCF7- RB-del
IgG
- + - +
IP:CDK2
T47D- WT
T47D- RB-del
IgG
- + - +
Palbo/Evero
CDK2
Cyclin E1
Cyclin A
pRB(S807/811)
RB Exo
Relative CDK2 kinase activity
MCF7-WT
MCF7-RB-del
DMSO
Palb/Evero
DMSO
Palb/Evero
Relative CDK2 kinase activity
T47D-WT
T47D-RB-del
DMSO
Palb/Evero
DMSO
Palb/Evero

B

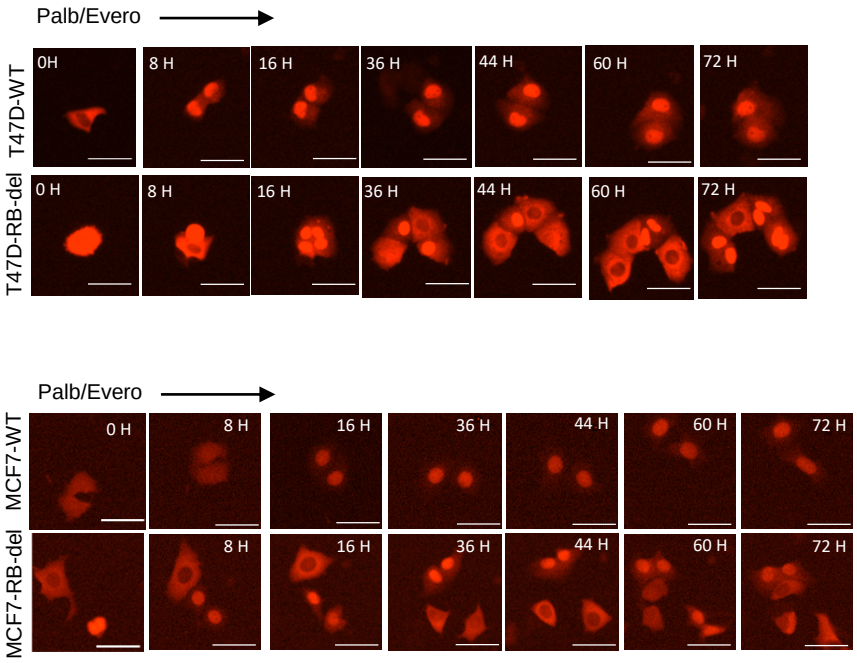
Palb/Evero
T47D-WT
0H
8 H
16 H
36 H
44 H
60 H
72 H
T47D-RB-del
0 H
8 H
16 H
36 H
44 H
60 H
72 H
Palb/Evero
MCF7-WT
0 H
8 H
16 H
36 H
44 H
60 H
72 H
MCF7-RB-del
8 H
16 H
36 H
44 H
60 H
72 H

A

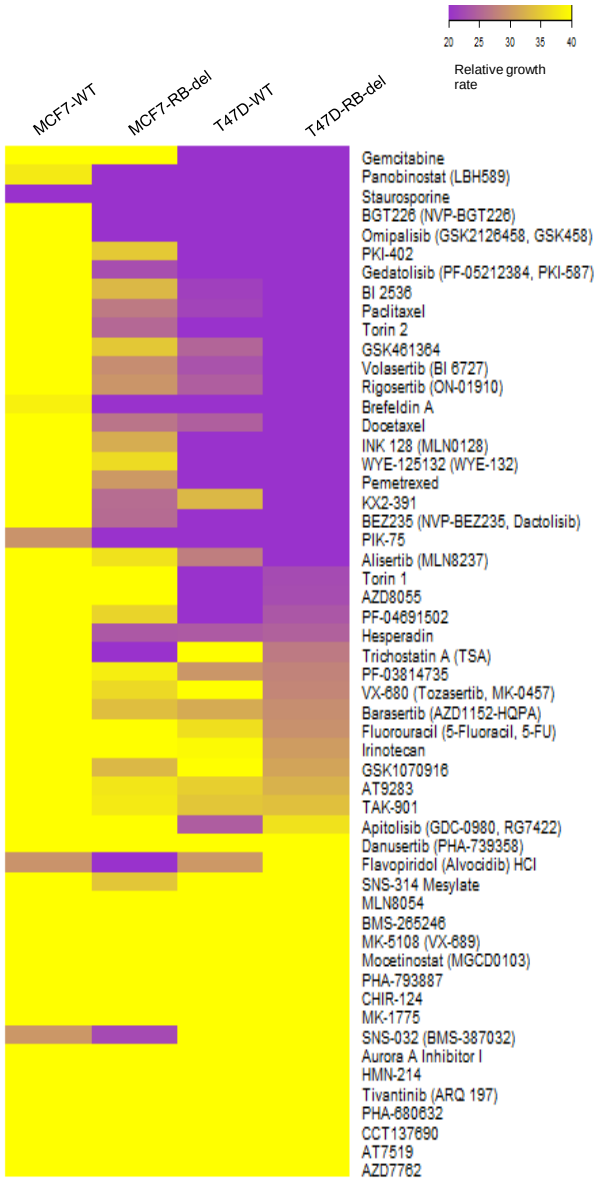

B

Drugs	Targets
Hesperadin	Aurora Kinase
TAK−901	
CCT137690	
SNS-314 Mesylate	
Danusertib (PHA−739358)	
MLN8054	
VX-680 (Tozasertib, MK-0457)	
Barasertib (AZD1152−HQPA)	
PF-03814735	
GSK1070916	
Aurora A Inhibitor I	
Alisertib (MLN8237)	
MK-5108 (VX-689)	
PHA-680632	
AT9283	
Rigosertib (ON-01910)	PLK
HMN-214	
BI 2536	
GSK461364	
Volasertib (BI 6727)	
PIK-75	DNA replication/synthesis
Doxorubicin (Adriamycin)	
Irinotecan	
Pemetrexed	
Gemcitabine	
Fluorouracil (5-Fluoracil, 5-FU)	
SNS-032 (BMS-387032)	CDK
Dinaciclib (SCH727965)	
AT7519	
Flavopiridol (Alvocidib) HCl	
AZD5438	
BMS-265246	
Milciclib (PHA-848125)	
PHA-793887	

C

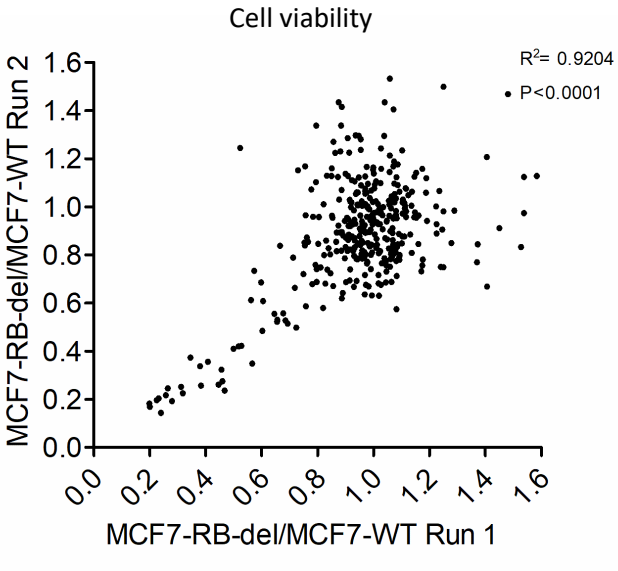

Fig S10

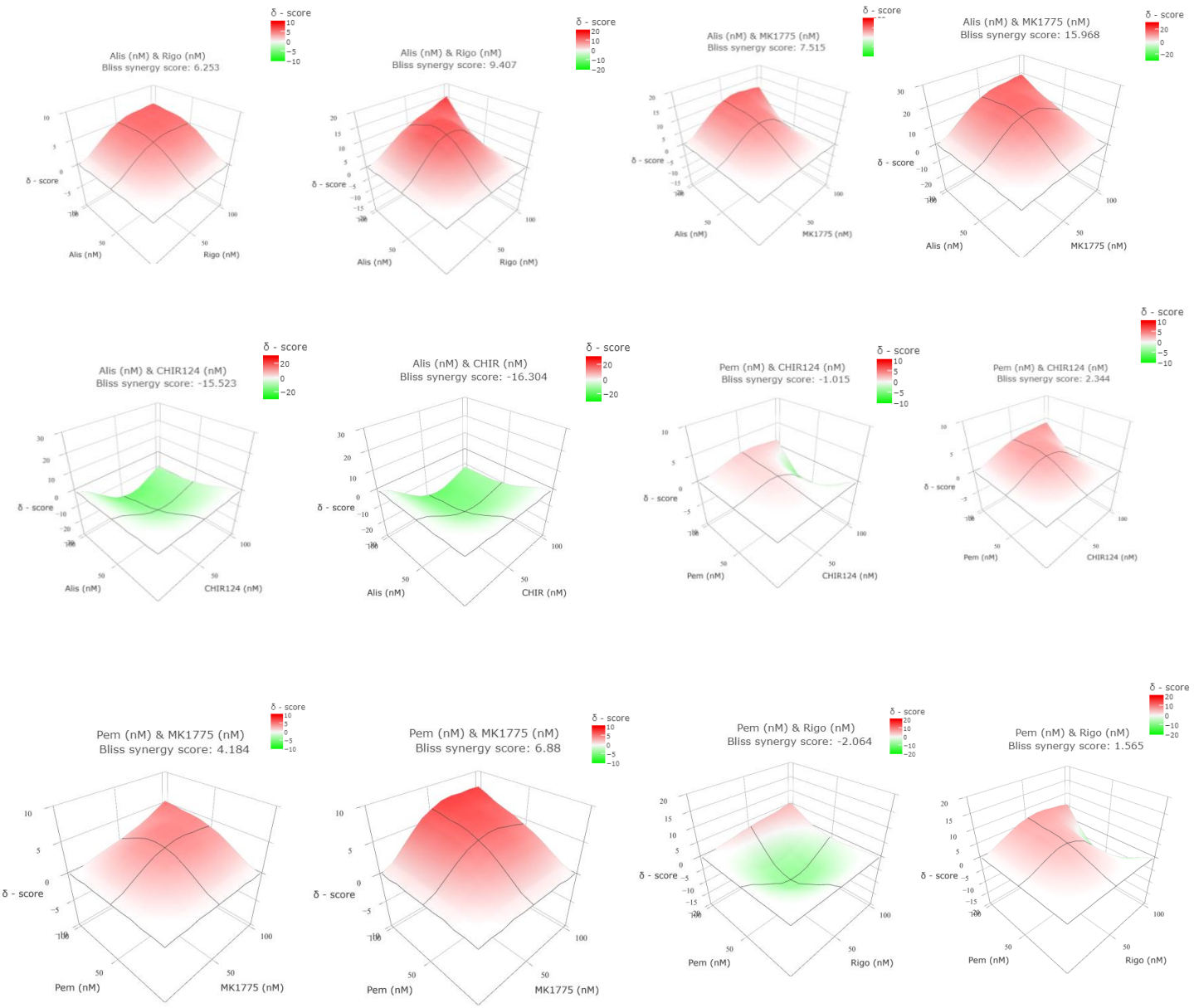
Alis (nM) & Rigo (nM)
Bliss synergy score: 6.253
Alis (nM) & Rigo (nM)
Bliss synergy score: 9.407
Alis (nM) & MK1775 (nM)
Bliss synergy score: 7.515
Alis (nM) & MK1775 (nM)
Bliss synergy score: 15.968
Alis (nM) & CHIR124 (nM)
Bliss synergy score: -15.523
Alis (nM) & CHIR (nM)
Bliss synergy score: -16.304
Pem (nM) & CHIR124 (nM)
Bliss synergy score: -1.015
Pem (nM) & CHIR124 (nM)
Bliss synergy score: 2.344
Pem (nM) & MK1775 (nM)
Bliss synergy score: 4.184
Pem (nM) & MK1775 (nM)
Bliss synergy score: 6.88
Pem (nM) & Rigo (nM)
Bliss synergy score: -2.064
Pem (nM) & Rigo (nM)
Bliss synergy score: 1.565
δ - score

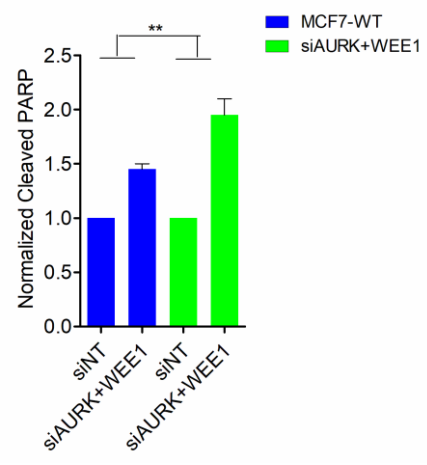
MCF7-WT
siAURK+WEE1
**
Normalized Cleaved PARP
2.5
2.0
1.5
1.0
0.5
0.0
siNT
siAURK+WEE1
siNT
siAURK+WEE1

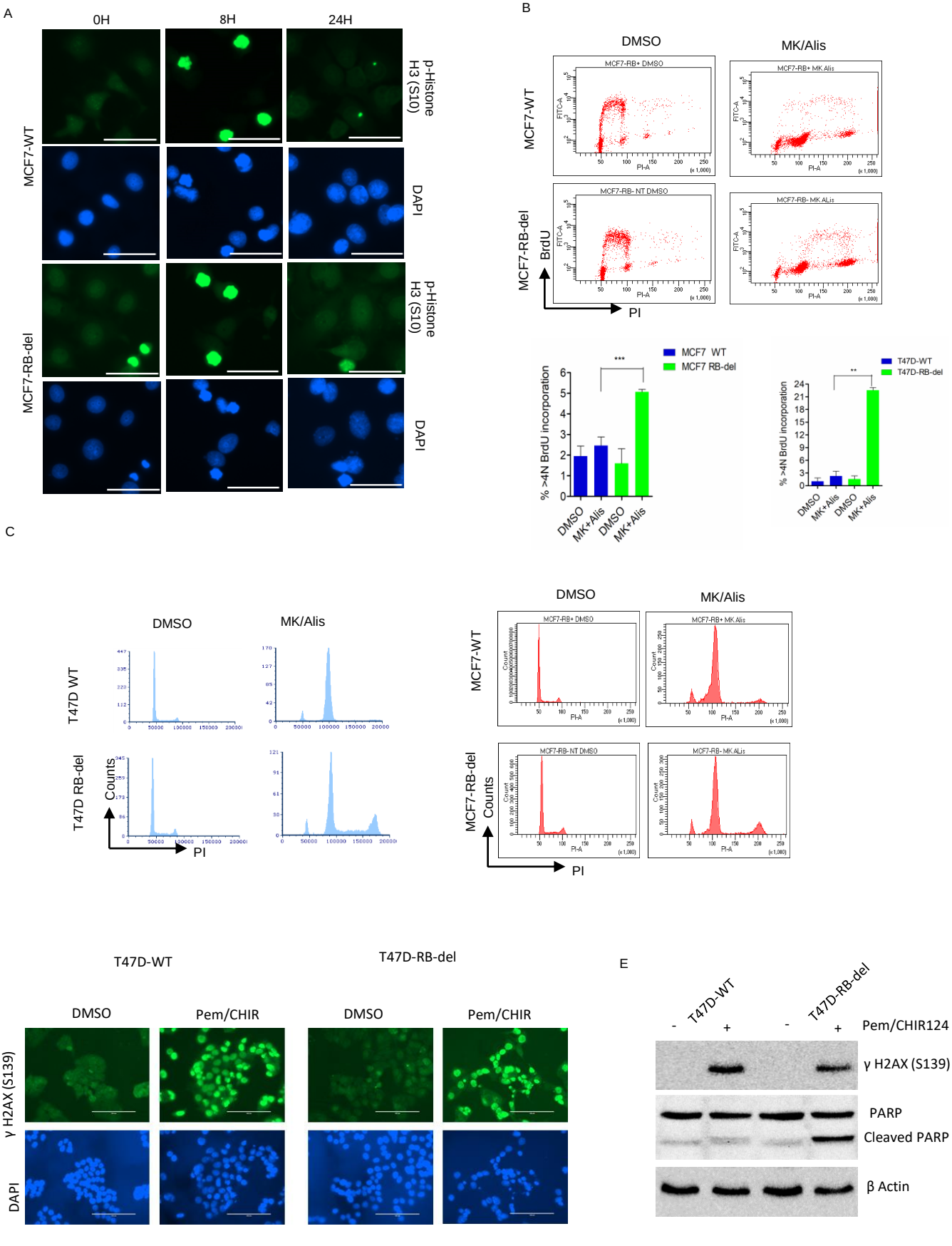
A
0H
8H
24H
MCF7-WT
MCF7-RB-del
p-Histone H3 (S10)
DAPI
B
DMSO
MK/Alis
MCF7-WT
MCF7-RB-del
BrdU
PI
MCF7-RB+ DMSO
MCF7-RB+ MK Alis
MCF7-RB- NT DMSO
MCF7-RB- MK ALis
MCF7 WT
MCF7 RB-del
T47D-WT
T47D-RB-del
% >4N BrdU incorporation
***
**
C
DMSO
MK/Alis
T47D WT
T47D RB-del
Counts
PI
MCF7-WT
MCF7-RB-del
D
T47D-WT
T47D-RB-del
DMSO
Pem/CHIR
γ H2AX (S139)
DAPI
E
T47D-WT
T47D-RB-del
Pem/CHIR124
γ H2AX (S139)
PARP
Cleaved PARP
β Actin

A

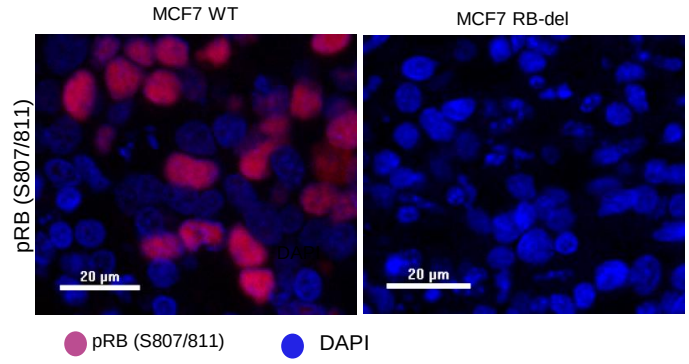
MCF7 WT
MCF7 RB-del
pRB (S807/811)
20 µm
20 µm
pRB (S807/811)
DAPI

B

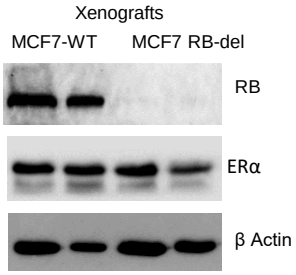
Xenografts
MCF7-WT
MCF7 RB-del
RB
ERα
β Actin

C

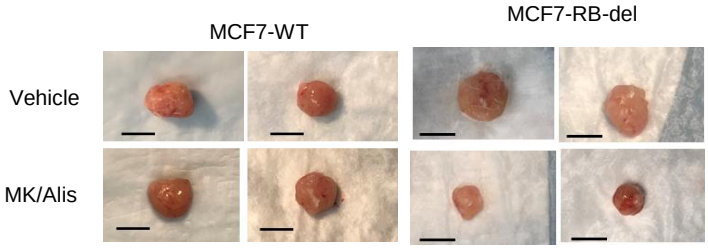
MCF7-WT
MCF7-RB-del
Vehicle
MK/Alis

D

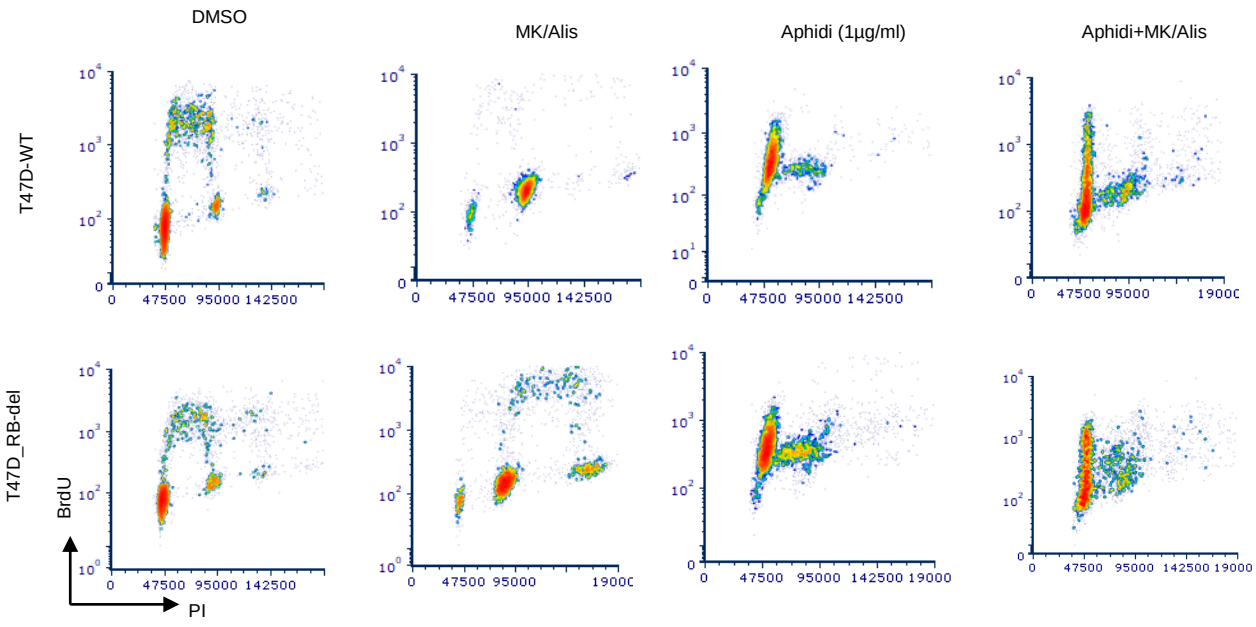
DMSO
MK/Alis
Aphidi (1µg/ml)
Aphidi+MK/Alis
T47D-WT
T47D_RB-del
BrdU
PI

E

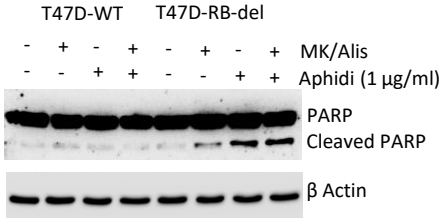
T47D-WT
T47D-RB-del
MK/Alis
Aphidi (1 µg/ml)
PARP
Cleaved PARP
β Actin

A

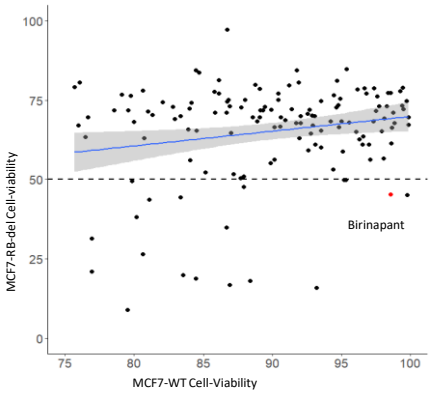
MCF7-RB-del Cell-viability
MCF7-WT Cell-Viability
Birinapant

B

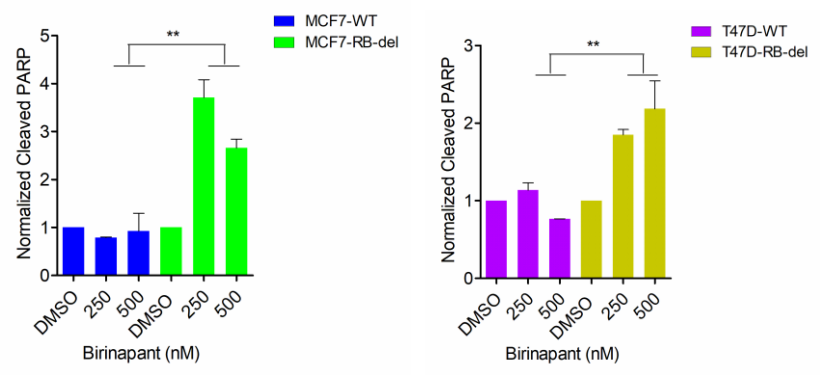
MCF7-WT
MCF7-RB-del
Normalized Cleaved PARP
Birinapant (nM)
DMSO
250
500
T47D-WT
T47D-RB-del

C

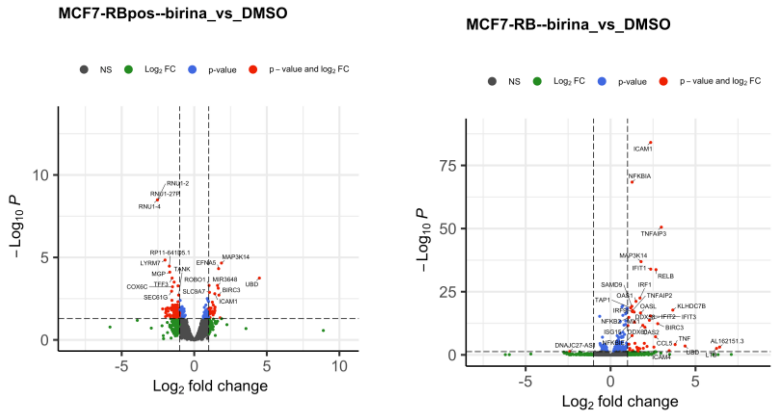
MCF7-RBpos--birina_vs_DMSO
MCF7-RB--birina_vs_DMSO
NS
Log2 FC
p-value
p – value and log2 FC
Log2 fold change

D

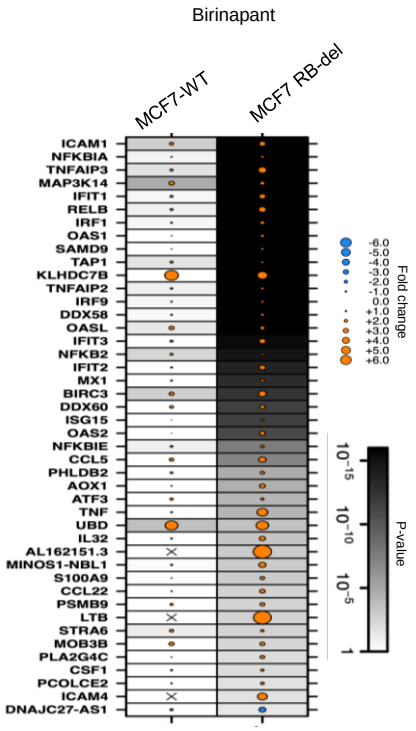
Birinapant
MCF7-WT
MCF7 RB-del
ICAM1
NFKBIA
TNFAIP3
MAP3K14
IFIT1
RELB
IRF1
OAS1
SAMD9
TAP1
KLHDC7B
TNFAIP2
IRF9
DDX58
OASL
IFIT3
NFKB2
IFIT2
MX1
BIRC3
DDX60
ISG15
OAS2
NFKBIE
CCL5
PHLDB2
AOX1
ATF3
TNF
UBD
IL32
AL162151.3
MINOS1-NBL1
S100A9
CCL22
PSMB9
LTB
STRA6
MOB3B
PLA2G4C
CSF1
PCOLCE2
ICAM4
DNAJC27-AS1
Fold change
P-value

E

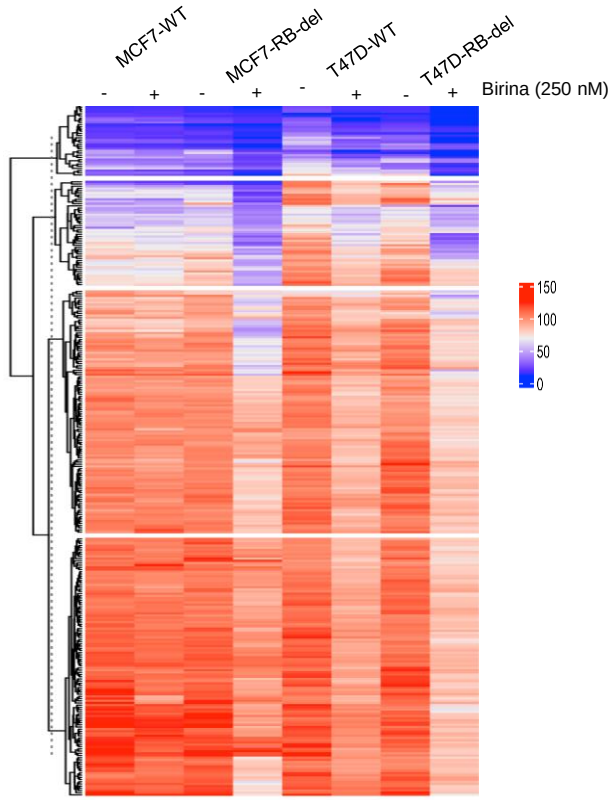
MCF7-WT
MCF7-RB-del
T47D-WT
T47D-RB-del
Birina (250 nM)